Springer

KSME

Journal of Mechanical Science and Technology 27 (5) (2013) 1393~1405
www.springerlink.com/content/1738-494x
DOI 10.1007/s12206-013-0320-7

Research on thermal deformation of large-scale computer numerical control gear hobbing machines †

Shilong Wang[1], Yong Yang[1,2,*], Xianguang Li[2], Jie Zhou[1] and Ling Kang[1]

[1]*The State Key Laboratory of Mechanical Transmission, Chongqing University, Chongqing 400044, China*
[2]*Chongqing Machine Tool (Group) Co., Ltd., Chongqing 400055, China*

(Manuscript Received April 23, 2011; Revised May 23, 2012; Accepted January 12, 2013)

Abstract

Research on thermal deformation of large-scale computer numerical control (CNC) hobbing machines is on the purpose of obtaining the law of thermal deformation of gear hobbing machines to improve machining precision. According to the structure characteristics of hobbing machines, this paper presents a novel computing model of thermal deformation based on the theory of the thermal expansion deformation of metallic materials, the extensional beam theory, non-uniform temperature distribution of the Euler-Bernoulli beam and Kirchhoff theory of plane-section assumption. Then, the coupling theory of axial and bending deformation of hobbing machines based on the deformation element and equilibrium element method is proposed. The experimental measurement system and platform for thermal deformation of gear hobbing machines is established. The temperature and displacement data of thermal deformation of a certain type gear hobbing machine is analyzed, which has demonstrated the law of thermal deformation of hobbing machines. The locus curves for overall displacement error of cutting points and teeth trace error are obtained. Comparing deformation theory and experimental data, the relative error is lower than 5%, which verifies the computing model proposed by this paper, and shows the research method has great significance for structural optimization, local temperature control, and prediction and compensation for thermal deformation error of gear hobbing machines.

Keywords: NC gear hobbing machines; Thermal deformation; Temperature; Cutting points; Experimental test; Error

1. Introduction

With the improvement of machine manufacturing level and the developing ability of gear hobbing machines, assembly and geometric error of tool machines are effectively controlled [1], and the thermal deformation during machining is the main source which causes workpiece errors [2]. Large-scale NC gear hobbing machines are used to make large, high precision gears for aircrafts, ships and engineering machines. Because of the large size of workpieces, the error is strongly related to thermal deformation of a machine tool. Thus, to improve the machining precision, a study of thermal deformation of large-scale NC gear hobbing machines is in urgent need.

Over the years, much work has been done to solve the problem concerned about effect of thermal deformation of machine tool on thermal error. Some achievement has been obtained in related theory, while little related experimental work and practical application have been reported. Okushima et al. [3] proposed using a linear, single variable mathematical model to determine the quantity relationship between temperature of key points and extension of the main spindle in milling machines, which started the quantitative studies on thermal deformation of machines. However, they did not make a formula deduction of thermal displacement and experimental verification. Tao et al. [4] made a simple deduction of thermal deviation of machine tool in terms of effect of thermal deformation on machining precision. But in this deduction the scale of temperature differences of machine tool was a bit large, as the unbalanced thermal distribution of machine tool was not taken into account and experimental verification was not done yet. Guan et al. [5] explored thermal deformation from cooling system, machining temperature and thermal radiation, and analyzed the effect of temperature on machining and measuring precision and did some work on temperature control. However, he did not deduce the formulas and no tests were done. Ju et al. [6] researched the application of composite components in machine tool deformation control. Through the characteristics of 2D heat transfer during phase change, they computed the temperature field and deformation of the column and main spindle of the machine tool, which are made of composite constant temperature materials, using adaptive

*Corresponding author. Tel.: +86 23 6510 3567, Fax.: +86 23 6510 6436 (801)
E-mail address: yangycqu@163.com
† Recommended by Associate Editor Chang-Wan Kim

variable grid finite element method. Nevertheless the related experiments were not done yet.

To uncover the thermal deformation law of large-scale NC gear hobbing machines, we conducted a theoretical study on displacement (in the direction of x-axis) from thermal deformation of the lathe bed and column considering the structure and heterogeneity of temperature distribution of gear hobbing machines. A novel computing model for thermal deformation displacement of a particular CNC gear hobbing machine is proposed. The change of cutting points and distance between centers of the hob and workpiece spindle is analyzed. As a research case, experiments for measuring temperature and displacement are conducted and comparison between theoretical displacement and experimental data are made.

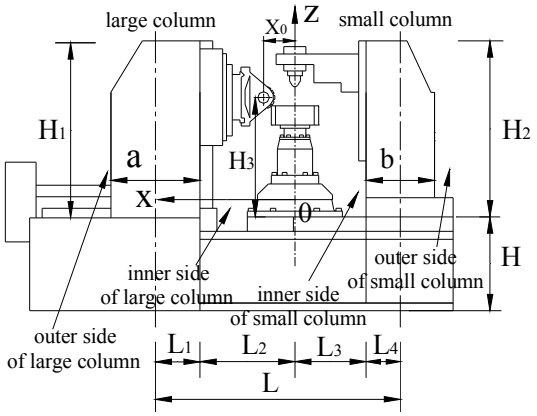

Fig. 1. Structure of NC gear hobbing machines.

2. Computing model for thermal deformation displacement of gear hobbing machines

The heat sources of gear hobbing machines include heat from surroundings and lightening, electrical motors, friction between rails, transmission mechanism, bearings and cutting heat. Among them, friction heat, cutting heat and heat from motors are the main sources of thermal deformation. Part of the heat generated in the machining process dissipates into the air, part of it is absorbed by the cooling fluid, and the rest of it is absorbed by the columns and lathe bed of the gear hobbing machines. But a large part of it is absorbed by the sprayed cooling fluid. As the working time of machining workpiece increases, the sprayed cooling fluid, cutting heat and heat from friction between rails and worm gear, which actuates the workbench to continue to heat the lathe bed and columns of the machine tool, especially the top surface of the lathe bed and inner side of columns. Because of the complexity of the structure of the machine tool, the heat distribution is not uniform, such as the temperature gradient from temperature difference between the top and bottom surface of the lathe bed of the gear hobbing machines, making the lathe bed bend upside and the columns incline to the direction of extension of the lathe bed. So the shift, inclination and bending of the column from thermal deformation cause the change of distance between centers of hob and workpiece spindle, leading to the offset in the contact between hob and cutting points (in the direction of x-axis or tooth trace error), which deteriorates the machining precision shown in Fig. 2. The diagram of a large-scale gear hobbing machine structure is in Fig. 1.

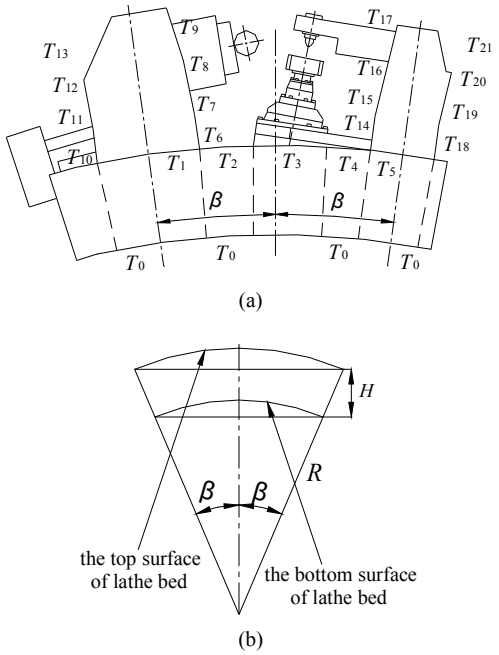

Fig. 2. Thermal deformation of NC gear hobbing machine: (a) Temperature distribution; (b) Thermal deformation of lathe bed.

2.1 The extension of lathe bed from thermal deformation

During the machining process, the cooling fluid is sprayed on the top surface of the lathe bed; cutting heat and friction heat in the rails and worm gears are all the main heat sources. Under this heat, the top surface of the lathe bed keeps being heated, which shows a temperature difference with the bottom surface, producing a temperature gradient between them. This causes the lathe bed to bend and extend upward. Due to the non-uniformity and complexity of heat distribution, and to ensure the exactness of calculating the thermal extension, the temperature measurement and computation of thermal extension is conducted in a sectional way.

As Fig. 2 shows, the top surface of the lathe bed is split into five sections; the average temperature of each is T_i ℃(i=5). Because the interior structure of the lathe bed is box body type and cooling fluid is cycled there, the temperature of the bottom surface of the lathe bed is almost the same, that is T_0 ℃. So the extension between centerlines of columns ΔL is

$$\Delta L = \sum_{i=1}^{5} \left(L_{i\exp} - L_i \right). \tag{1}$$

According to Figs. 1 and 2, the thermal extension between centerlines of columns is computed in a sectional way. The

coefficient of heat expansion of materials of the lathe bed and columns is λ, and elasticity modulus is E.

Based on the heat expansion theory of metal [7, 8], the relationship function between thermal extension of the *i*th section of the lathe bed and change of temperature is

$$\frac{dL_i}{L_i} = \lambda dT_i \qquad (i = 5). \tag{2}$$

From Eq. (2)

$$L_{i\exp} = L_i e^{\lambda(T_i - T_0)} \qquad (i = 5). \tag{3}$$

From Eqs. (1) and (3), the thermal extension between centerlines of columns is

$$\Delta L = \sum_{i=1}^{5} L_i[\mathrm{e}^{\lambda(\mathrm{T_i}-\mathrm{T_0})}\text{-}1]. \tag{4}$$

2.2 The variation between distance of centers of hob and workpiece spindle from inclination of the columns

The large column is assembled on the left side of the top surface of the lathe bed vertically, and the smaller one is assembled on the right. The large column can be moved horizontally along the horizontal rails which hold the position in the process of cutting. Outer brackets, ejector pins of spindle and extruding part of workbench are all installed on the small column, while the hob box (including the slide, motor, transmission mechanism, hob bracket, the spindle, hob rod and hob etc.) is on the large column. Thus, when the lathe bed is bent upwards from thermal extension, both of the columns will incline outward individually, and the hob spindle inclines with the large column, while the workpiece spindle with the smaller one. The distance between centers of the hob and workpiece spindles at the height of H_3 above cutting points caused by inclination of the columns can be computed through position change of the hob and workpiece spindles. Considering that the strength and stiffness of the machine tool is enough, and the extension from thermal deformation is very small, so the angles of inclination between the center line of the large column or small column and vertical line are all small. To simplify the deduction, we set both the angles of inclination to be the same, denoted by β, so the angles of inclination of spindles of the hob and workpiece are approximately β, as is shown in Figs. 2 and 3. The inclination of the hob and workpiece spindles makes the distance of centers increase. Because the stiffness of the materials of the gear hobbing machines is sufficient enough, the sum of the *x* direction component displacement of the inclination of the two spindles at the height of H_3 is the variation of the distance of centers, which is also the offset of the position of cutting points causing errors of machining gear. For the convenience of demonstration and research, we extend the center axis of hob to intersect with the bed, as is shown in Fig. 3, which

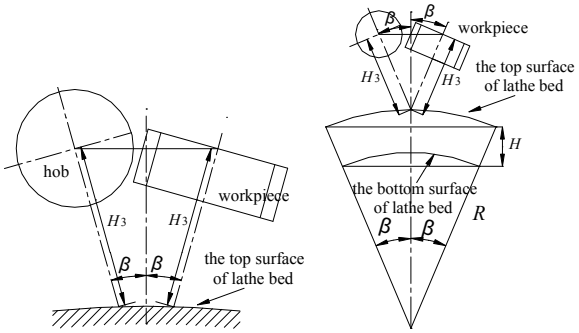

Fig. 3. Inclination of hob and workpiece spindle.

simplifies structure of the hob and workpiece spindle. The hob and workpiece spindles are described by the centerline, the positions of which will show the variation.

Due to the stiffness of the columns being sufficient enough, and the same angles of inclination, so the *x* direction component displacements of the columns at the height of H_3 are equal, which means the offset in the direction of the *x* axis should be the same. The sum of the two offsets will be the variation of the center distance of the two spindles, whose formula is [3]

$$\Delta S = \Delta S_{\mathrm{a}} + \Delta S_{\mathrm{b}} = \frac{\Delta S}{2} + \frac{\Delta S}{2} = 2H_3 \sin\beta \tag{5}$$

where ΔS is the variation of distance of centers of the two spindles (*x* offset of cutting point), ΔS_{a} is *x* offset which causes inclination of large column, ΔS_{b} is the *x* offset which causes inclination of small column, H_3 is the height of cutting point above the lathe bed, and 2β is the central angle between the both centerlines of the hob and workpiece spindles.

According to Figs. 2 and 3,

$$\frac{L}{L+\Delta L} = \frac{R\left[1-(\sin\beta)^2\right]^{\frac{1}{2}} - H}{R\left[1-(\sin\beta)^2\right]^{\frac{1}{2}}} \tag{6}$$

$$2\pi R \times \frac{2\beta}{2\pi} = \hat{L} \tag{7}$$

where R is the bend radius of the top surface of lathe bed arising from thermal deformation. For a very small value of β, by the principle of series convergence, we can obtain

$$\sqrt{1-(\sin\beta)^2} = \left(1-\beta^2\right)^{\frac{1}{2}} = 1 - \frac{1}{2}\beta^2. \tag{8}$$

Substituting Eq. (8) into Eq. (6), Eqs. (5) and (6) can be simplified:

$$\Delta S = 2H_3\beta \tag{9}$$

$$\frac{L}{L+\Delta L} = \frac{R\left(2-\beta^2\right) - 2H}{R\left(2-\beta^2\right)} \tag{10}$$

$$2\beta R = L + \Delta L . \tag{11}$$

Substituting Eq. (10) into Eq. (11) becomes

$$\Delta L\beta^2 + 4H\beta - 2\Delta L = 0 . \tag{12}$$

Solving Eq. (12), the result is

$$\beta = \frac{2}{\Delta L} \times \left[\left(H^2 + \frac{1}{2}\Delta L^2 \right)^{\frac{1}{2}} - H \right] . \tag{13}$$

Substituting Eq. (4) in Eq. (13):

$$\beta = 2\frac{\left\{ H^2 + \frac{1}{2}\left\{ \sum_{i=1}^{5} L_i \left[e^{\lambda(T_i - T_0)} - 1 \right] \right\}^2 \right\}^{\frac{1}{2}} - H}{\sum_{i=1}^{5} L_i \left[e^{\lambda(T_i - T_0)} - 1 \right]} . \tag{14}$$

Substituting Eq. (14) into Eq. (9), the variation of distance of centers of the hob and workpiece spindles arising from the inclination of two columns at height of H_3 can be obtained

$$\Delta S = 4H_3 \times \frac{\left\{ H^2 + \frac{1}{2}\left\{ \sum_{i=1}^{5} L_i \left[e^{\lambda(T_i - T_0)} - 1 \right] \right\}^2 \right\}^{\frac{1}{2}} - H}{\sum_{i=1}^{5} L_i \left[e^{\lambda(T_i - T_0)} - 1 \right]} . \tag{15}$$

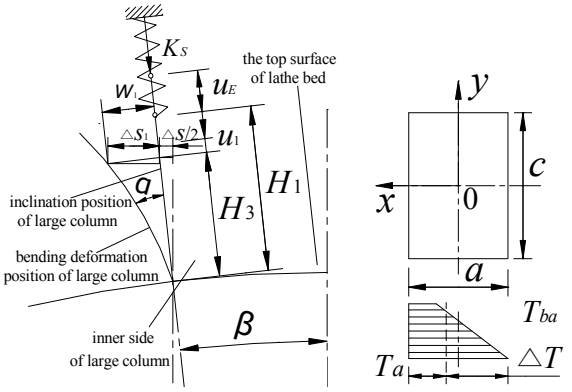

Fig. 4. Bend thermal deformation and cross-section temperature distribution of the large column of CNC gear hobbing machines.

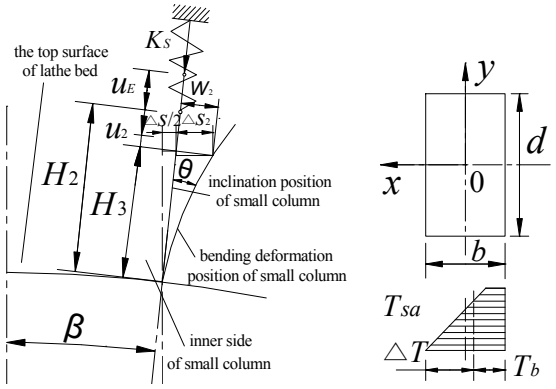

Fig. 5. Bend thermal deformation and cross-section temperature distribution of the small column of CNC gear hobbing machines.

2.3 The variation of distance of centers of the hob and workpiece spindles caused by thermal deformation of bend of the columns

Because of uneven distribution of temperature of the columns, this will produce thermal bending and second order bending moment. Meanwhile, yield strength and elasticity modulus are also distributed unevenly. The centroid of cross section of the column will move to the colder side. With the hob box on the large column and outer bracket on the smaller one, when finishing gear cutting and unloading the gear, both the hob box and outer bracket will slide along the rails of the columns themselves, plus cutting force will exert axial load to the column, so the column can be treated as the component under axial compression with uneven temperature distribution. The temperature difference between inner and outer side of column will form a temperature gradient, which will affect the axial load on the column [9, 10]. Because the end of the column is fixed on the bed, the thermal deformation causes the inclination of the column; the temperature gradient makes the axial load change significantly, leading to the bending of the column.

During the process of gear cutting and unloading gears and loading workpieces, the hob box and outer bracket will move upwards and downwards repeatedly, which has the effect of a periodic variation of axis load. To establish the balanced equation, assume an axial elastic constraint is set on the top of the column, then the thermal bending of the column can be treated as the simple beam with a elastic axial constraint on the top, as is shown in Figs. 4 and 5. For the sake of study, the position change caused by the thermal deformation of the column can be shown from the position change of the centerline. So the following sketch will only show the centerlines. The bending of the column will lead to the change of the distance of centers of hob and workpiece spindles, which causes the position change of cutting points and machining error.

According to the theory of extending of axis, if a column with uneven temperature distribution obeys the Euler-Bernoulli beam theory and Kirchhoff assumption of cross section, we can only consider the bending of column around the axis, without consideration of the effect of bending outside of plane and local bending [11, 12]. Because the column bears the axial load and thermal expansion, the bending of the column can be seen as the coupled effect of axial deformation and bending [13]. To solve the problem of bending of a large column at the state of heat balance, evaluate the deformation element and equilibrium element, as is shown in Fig. 6.

The point $P(0, z)$ on the centerline of the column before

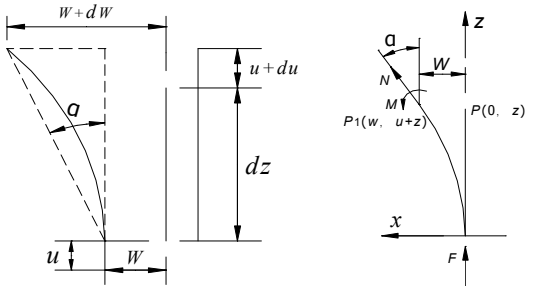

Fig. 6. Thermal deformation bends of deformation element and equilibrium element of large column: (a) Deformation element; (b) Equilibrium element.

thermal deformation moves to the point $P_1(w\ ,\ u+z)$ after bending, where $u = u(z)$ and $w = w(z)$ are the displacement of the point P along the z axis and x axis, as is shown in Fig. 6. According to the beam theory of extending axis [14],

$$\varepsilon = \varepsilon_0 - x\cdot\phi - \varepsilon_{th} \quad (-\frac{a}{2}\le x\le\frac{a}{2}) \tag{16}$$

$$\varepsilon_0 = \sqrt{\left(1+\frac{du}{dz}\right)^2+\left(\frac{dW}{dz}\right)^2}-1 \tag{17}$$

$$\phi = \frac{\dfrac{dW}{dz}\left(\dfrac{d^2u}{dz^2}\right)-\dfrac{d^2W}{dz^2}\left(1+\dfrac{du}{dz}\right)}{\left[\left(1+\dfrac{du}{dz}\right)+\dfrac{dW}{dz}\right]^{\frac{3}{2}}} \tag{18}$$

$$\varepsilon_{th} = \lambda T \tag{19}$$

$$\cos\alpha = \left(1+\frac{du}{dz}\right)\Big/\sqrt{\left(1+\frac{du}{dz}\right)^2+\left(\frac{dW}{dz}\right)^2}\ . \tag{20}$$

During the process of gear cutting, the deflection from axial load and temperature gradient is very small, so the column can be considered to be made of materials with linear thermal elasticity, and the relationship between stress and strain is

$$\sigma = E\varepsilon \tag{21}$$

$$T = T_c + k\cdot x \quad (-\frac{a}{2}\le x\le\frac{a}{2}). \tag{22}$$

As Fig. 2 shows, the temperature of inner and outer side of the large column is taken as the average temperature. The result is

$$T_{ba} = \frac{1}{4}\sum_{i=6}^{9}T_i\ ,\quad T_a = \frac{1}{4}\sum_{i=10}^{13}T_i\ ,\quad T_c = \frac{T_{ba}+T_a}{2}$$

$$\Delta T = \frac{T_{ba}-T_a}{2} = \frac{1}{8}\left(\sum_{i=6}^{9}T_i - \sum_{i=10}^{13}T_i\right) \tag{23}$$

$$k = \frac{\Delta T}{a/2} = \frac{(T_{ba}-T_a)}{a} \tag{24}$$

where α is the rotation angle of the cross section of the column, ε_0 is the axial strain at the centroid of cross section of the column, ε is the normal strain of the arbitrary point on the cross section of the column, ε_{th} is the thermal strain of arbitrary point, T is the temperature of arbitrary point, T_c is the temperature of the centroid of cross section of the column, T_a is the average temperature of outer side of large column, T_{ba} is the average temperature of inner side of large column, ΔT is the temperature difference of between edge and centroid of the cross section of large column, k is the temperature gradient (the temperature change of unit length between inner side and outer side of large column), and x is the distance from any point to center.

As the equilibrium element body in Fig. 6, the balance equations of the axial load of the column are

$$F\cdot\cos\alpha + N = 0 \tag{25}$$

$$F\cdot W + M = 0 \tag{26}$$

$$F = F_0 + K_s\cdot\left(u_E + \frac{F_0}{K_c}\right) \tag{27}$$

$$N = \iint_A \sigma dA\ ,\quad M = \iint_A \sigma x dA \tag{28}$$

where $F_0 = \eta\sigma_s A$, $K_c = EA/H_1$, $K_s = \xi K_C$, σ is the stress of arbitrary point of large column, F_0 is the axial force of large column in the original design, η is load ratio, σ_s is the yielding strength at the room temperature, A is the area of cross section of large column, K_c is the stiffness of pull pressure, K_s is the stiffness of elastic axial constraint, ξ is the stiffness ratio of elastic axial constraint, and u_E is the deformation displacement of top of large column.

According to Eqs. (22)-(24)

$$T = \frac{T_{ba}+T_a}{2} + \frac{T_{ba}-T_a}{a}\cdot x\ (-\frac{a}{2}\le x\le\frac{a}{2}). \tag{29}$$

According to Eqs. (16)-(19), (21), (28) and (29),

$$N = EA\left(\sqrt{\left(1+\frac{du}{dz}\right)^2+\left(\frac{dW}{dz}\right)^2}-1-\lambda T_c\right) \tag{30}$$

$$M = EI\left\{\frac{\dfrac{dW}{dz}\dfrac{d^2u}{dz^2}-\dfrac{d^2W}{dz^2}\left(1+\dfrac{du}{dz}\right)}{\left[\left(1+\dfrac{du}{dz}\right)^2+\left(\dfrac{dW}{dz}\right)^2\right]^{\frac{3}{2}}}-\frac{2\lambda\Delta T}{a}\right\}. \tag{31}$$

According to Eqs. (20), (25)-(27), (30) and (31),

$$12W\left(\sqrt{\left(1+\frac{du}{dz}\right)^2+\left(\frac{dW}{dz}\right)^2}-1+\lambda T_c\right)\times$$

$$\left[\left(1+\frac{du}{dz}\right)^2+\left(\frac{dW}{dz}\right)^2\right]^2 = a^2\left(1+\frac{du}{dz}\right)\times\left\{\frac{dW}{dz}\frac{d^2u}{dz^2}\right.$$

$$-\frac{d^2W}{dz^2}\left(1+\frac{du}{dz}\right)-\frac{2\Delta T\lambda}{a}\left[\left(1+\frac{du}{dz}\right)^2+\left(\frac{dW}{dz}\right)^2\right]^{\frac{3}{2}}\Bigg\},$$

$$(0\le z\le H_3). \tag{32}$$

According to Eqs. (26), (27) and (31),

$$W\left[\eta A\sigma_s(1+\xi)+\xi\frac{EAu_E}{H_1}\right]=$$
$$EI\left\{\frac{2\lambda\Delta T}{a}-\frac{\dfrac{dW}{dz}\dfrac{d^2u}{dz^2}-\dfrac{d^2W}{dz^2}\left(1+\dfrac{du}{dz}\right)}{\left[\left(1+\dfrac{du}{dz}\right)^2+\left(\dfrac{dW}{dz}\right)^2\right]^{\frac{3}{2}}}\right\}. \tag{33}$$

According to the assembling of the column of large-scale CNC hobbing machines, the geometric boundary condition of axis deflection and bending deflection u and W is

$$u\big|_{z=0}=0,\quad u\big|_{z=H_3}=u_1,\quad W\big|_{z=0}=0,W\big|_{z=H_3}=W_1.$$

With the conditions of minimum error for geometric boundary and control differential equations of bending of column from thermal deformation, the coefficients of the polynomial are determined by nonlinear least squares [15]. When the load ratio $\eta=0$, $\xi=0$, the solutions of Eqs. (32) and (33) are

$$u=\frac{a}{2\lambda\cdot\Delta T}\sin\left\{\frac{2\lambda\cdot\Delta T}{a}\left[1+\frac{\lambda(T_{ba}+T_a)}{2}\right](z-H_3)\right\}$$
$$-z+\frac{a}{2\lambda\cdot\Delta T}\sin\left\{\frac{2\lambda\cdot\Delta T\cdot H_3}{a}\left[1+\frac{\lambda(T_{ba}+T_a)}{2}\right]\right\} \tag{34}$$

$$W=\frac{a}{2\lambda\cdot\Delta T}\cos\left\{\frac{2\lambda\cdot\Delta T}{a}\left[1+\frac{\lambda(T_{ba}+T_a)}{2}\right](z-H_3)\right\}$$
$$-\frac{a}{2\lambda\cdot\Delta T}\cos\left\{\frac{2\lambda\cdot\Delta T\cdot H_3}{a}\left[1+\frac{\lambda(T_{ba}+T_a)}{2}\right]\right\}. \tag{35}$$

When $\frac{\lambda\cdot\Delta T}{a}\left[1+\frac{\lambda(T_{ba}+T_a)}{2}\right]$ is small, according to the convergence theory of power series, the axial thermal deformation and bending at the height of H_3 on the large column are

$$u_1=\frac{\lambda H_3(T_{ba}+T_a)}{2}=\frac{\lambda H_3\frac{1}{4}\left(\sum_{i=6}^{9}T_i+\sum_{i=10}^{13}T_i\right)}{2}$$
$$=\frac{\lambda H_3\left(\sum_{i=6}^{9}T_i+\sum_{i=10}^{13}T_i\right)}{8} \tag{36}$$

$$W_1=\frac{\lambda\Delta TH_3^2}{a}\left[1+\frac{\lambda(T_{ba}+T_a)}{2}\right]^2=\frac{\lambda H_3^2(T_{ba}-T_a)}{2a}\times\left[1+\frac{\lambda(T_{ba}+T_a)}{2}\right]^2$$
$$=\frac{\lambda H_3^2\frac{1}{4}\left(\sum_{i=6}^{9}T_i-\sum_{i=10}^{13}T_i\right)}{2a}\times\left[1+\frac{\lambda\frac{1}{4}\left(\sum_{i=6}^{9}T_i+\sum_{i=10}^{13}T_i\right)}{2}\right]^2$$
$$=\frac{\lambda H_3^2\left(\sum_{i=6}^{9}T_i-\sum_{i=10}^{13}T_i\right)}{8a}\times\left[1+\frac{\lambda\left(\sum_{i=6}^{9}T_i+\sum_{i=10}^{13}T_i\right)}{8}\right]^2. \tag{37}$$

Because the stiffness and strength of linking components of hob and column spindles are sufficient by the analysis in section 1.2, the x direction component of bending of large column is the part of variation of distance between centers of two spindles, which causes the machining error. According to Fig. 4, Eqs. (14), (20), (36) and (37), the deflection and rotation angle of the cutting point at the height of H_3 on the large column are

$$\Delta S_1=W_1\cos\beta$$
$$\Delta S_1=\frac{\lambda H_3^2\left(\sum_{i=6}^{9}T_i-\sum_{i=10}^{13}T_i\right)}{8a}\times\left[1+\frac{\lambda\left(\sum_{i=6}^{9}T_i+\sum_{i=10}^{13}T_i\right)}{8}\right]^2\times$$
$$\left\{1-2\left\{\frac{\left\{H^2+\frac{1}{2}\left\{\sum_{i=1}^{5}L_i\left[e^{\lambda(T_i-T_0)}-1\right]\right\}^2\right\}^{\frac{1}{2}}-H}{\sum_{i=1}^{5}L_i\left[e^{\lambda(T_i-T_0)}-1\right]}\right\}^2\right\} \tag{38}$$

$$\alpha=\frac{2\lambda\Delta TH_3(1+\lambda T_c)}{a}$$
$$=\frac{\lambda H_3\left(\sum_{i=6}^{9}T_i-\sum_{i=10}^{13}T_i\right)}{4a}\left[1+\frac{\lambda\left(\sum_{i=6}^{9}T_i+\sum_{i=10}^{13}T_i\right)}{4}\right]. \tag{39}$$

Similarly, the position deflection and rotation angel of cutting point at the height of H_3 of small columns are

$$\theta=\frac{2\lambda\Delta TH_3(1+\lambda T_c)}{b}$$
$$=\frac{\lambda H_3\left(\sum_{i=14}^{17}T_i-\sum_{i=18}^{21}T_i\right)}{4b}\left[1+\frac{\lambda\left(\sum_{i=14}^{17}T_i+\sum_{i=18}^{21}T_i\right)}{4}\right] \tag{40}$$

$$\Delta S_2=\frac{\lambda H_3^2\left(\sum_{i=14}^{17}T_i-\sum_{i=18}^{21}T_i\right)}{8b}\times\left[1+\frac{\lambda\left(\sum_{i=14}^{17}T_i+\sum_{i=18}^{21}T_i\right)}{8}\right]^2\times$$
$$\left\{1-2\left\{\frac{\left\{H^2+\frac{1}{2}\left\{\sum_{i=1}^{5}L_i\left[e^{\lambda(T_i-T_0)}-1\right]\right\}^2\right\}^{\frac{1}{2}}-H}{\sum_{i=1}^{5}L_i\left[e^{\lambda(T_i-T_0)}-1\right]}\right\}^2\right\}. \quad (41)$$

Through the analysis above, the sum of position deflection at the height of H_3 from thermal deformation of both the columns $\Delta S_1+\Delta S_2$ is the variation of distance between centers of two spindles, which is also the position deflection of the cutting point.

3. The position offset of cutting point caused by thermal deformation of hobbing machines

Through the analysis above, the position deviation of cutting point consists of the following three aspects:

(1) Because the stiffness and strength of the whole machine tool is sufficient the sum (ΔL) of outer offset of large and small columns is the extension of thermal deformation of the lathe bed. The hob box (with the hob spindle assembled on the hob box) is fixed on the large column. Outer bracket, mandrel of the workpiece and extruding part of worktable are all fixed on the small column, so the offset of distance of centers of the hob and workpiece spindles caused by thermal deformation equals approximately the sum (ΔL) of offsets of both columns. Thus the offset of cutting point caused by thermal extension equals the sum (ΔL) of offset of the distance of centers of the two spindles, which is the offset of the cutting point caused by thermal deformation of the lathe bed.

(2) From the analysis in section 1.2, the sum (ΔS) of offsets of cutting point equals approximately the sum of variation of distance of centers between the hob and workpiece spindles caused by the inclination of columns.

(3) From the analysis in section 1.3, the sum of offsets of cutting point caused by the thermal deformation of bending of two columns is almost the same as the sum ($\Delta S_1+\Delta S_2$) of offsets of the distance of centers between the hob and workpiece spindles.

Thus, under the sufficient stiffness and strength of gear hobbing machines, the sum Δx of offsets of distance of centers between the hob and workpiece spindles at the height of H_3, Δx is the sum of offsets of cutting point (named by thermal error or the tooth trace deviation). (This paper will omit the error of cutting point thermal error of the hob and workpiece spindles, bending deformation caused by cutting force, and the deformation of thermal expansion of the hob and workpiece due to their small value.) And the rotation angle between the two spindles centerline is also the sum of angles from the three aspects above.

According to Eqs. (14), (15), (38) and (40), the sum of offsets Δx at the height of H_3 above the cutting point caused by thermal deformation is

$$\Delta x=\Delta L+\Delta S+\Delta S_1+\Delta S_2=$$
$$\Delta L+4H_3\times\frac{\left[H^2+\frac{1}{2}(\Delta L)^2\right]^{0.5}-H}{\Delta L}+$$
$$\left\{\frac{\lambda H_3^2\left(\sum_{i=6}^{9}T_i-\sum_{i=10}^{13}T_i\right)}{8a}\times\left[1+\frac{\lambda\left(\sum_{i=6}^{9}T_i+\sum_{i=10}^{13}T_i\right)}{8}\right]^2\times\right.$$
$$\left.\left\{1-2\left\{\frac{\left[H^2+\frac{1}{2}(\Delta L)^2\right]^{0.5}-H}{\Delta L}\right\}^2\right\}\right\}$$
$$+\left\{\frac{\lambda H_3^2\left(\sum_{i=14}^{17}T_i-\sum_{i=18}^{21}T_i\right)}{8b}\times\left[1+\frac{\lambda\left(\sum_{i=14}^{17}T_i+\sum_{i=18}^{21}T_i\right)}{8}\right]^2\times\right.$$
$$\left.\left\{1-2\left\{\frac{\left[H^2+\frac{1}{2}(\Delta L)^2\right]^{0.5}-H}{\Delta L}\right\}^2\right\}\right\} \quad (42)$$

where $\Delta L=\sum_{i=1}^{5}L_i[e^{\lambda(T_i-T_0)}-1]$.

From Eqs. (14), (39) and (41), the angle φ between the hob and workpiece spindle centerlines is

$$\phi=2\beta+\alpha+\theta=4\frac{\left\{H^2+\frac{1}{2}(\Delta L)^2\right\}^{\frac{1}{2}}-H}{\Delta L}$$
$$+\frac{\lambda H_3\left(\sum_{i=6}^{9}T_i-\sum_{i=10}^{13}T_i\right)}{4a}\times\left[1+\frac{\lambda\left(\sum_{i=6}^{9}T_i+\sum_{i=10}^{13}T_i\right)}{4}\right] \quad (43)$$
$$+\frac{\lambda H_3\left(\sum_{i=14}^{17}T_i-\sum_{i=18}^{21}T_i\right)}{4b}\times\left[1+\frac{\lambda\left(\sum_{i=14}^{17}T_i+\sum_{i=18}^{21}T_i\right)}{4}\right].$$

4. The experiment of measuring thermal deformation and temperature of gear hobbing machines

4.1 Principle of experiment

Patch platinum resistance type temperature sensors are used to measure the temperature of inner and outer surface of col-

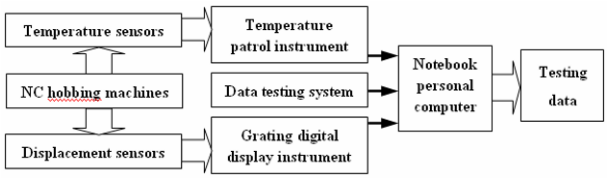

Fig. 7. Experiment principle of thermal deformation.

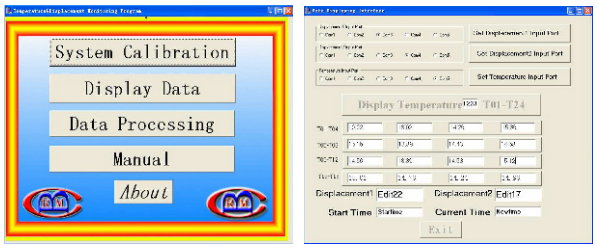

Fig. 8. Interface of experimental data Testing system.

umns, top and bottom surface of lathe bed. Grating displacement sensors are used to measure the displacement of bottom and top end of inner side of column, as is shown in Fig. 7. The experimental data of temperature and thermal deformation is acquired through the temperature patrol instrument and grating digital display instrument with the R232 serial port. The test system of temperature and displacement is developed by C++, and the data will be shown and saved to the computer automatically. The interface of the test system is shown in Fig. 8.

4.2 The testing method of thermal deformation displacement

Due to the sufficient stiffness and omission of thermal expansion of the lathe bed and columns, the extension ΔL between centerlines of both columns can be replaced with the sum of displacement at the bottom of inner side of both columns. The measurement of ΔL is

$$\Delta L = \Delta x_1 + \Delta x_2 \tag{44}$$

where Δx_1 is the measured value of displacement at the bottom of inner side of large column, Δx_2 is the measured value of displacement at the bottom of inner side of small column. Unit adopted is: mm.

Due to the sufficient column stiffness, the displacement caused by the inclination and bending deformation of large column is acquired by measuring the displacement Δx_5 at the top of large column. The displacement Δx_3 at the height of H_3 caused by inclination and bending deformation of large column can be obtained by triangle similarity theory (see Fig. 9(a)). So

$$\frac{\Delta S}{2} + \Delta S_1 = \Delta x_3 \tag{45}$$

$$\frac{\Delta x_3}{\Delta x_5} = \frac{H_3}{H_{11}} \Rightarrow \Delta x_3 = \frac{H_3}{H_{11}} \Delta x_5 \tag{46}$$

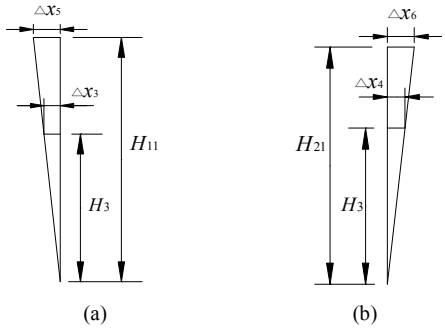

Fig. 9. Displacement measure and data transform of column top: (a) Large column top; (b) Small column top.

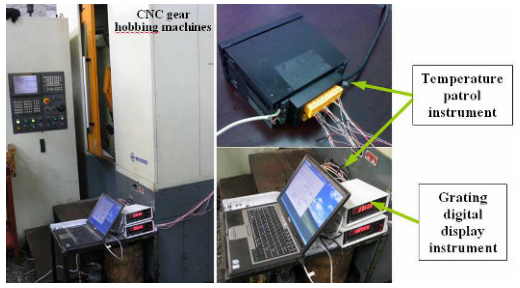

(a)

(b)

Fig. 10. Testing layout of thermal deformation experiment: (a) Layout of testing system; (b) Layout of temperature sensors.

where $\Delta S/2$ is the displacement of the hob spindle at the height of H_3 caused by inclination deformation of the large column, ΔS_1 is the displacement of the hob spindle at the height of H_3 caused by bending deformation of the large column, Δx_3 is the displacement of the hob spindle at the height of H_3 caused by inclination and bending deformation of the large column, Δx_5 is the measured value of displacement at the top of large column. H_{11} is the height of grating displacement sensor to the top surface of the lathe bed (see Fig. 12(a)). Unit adopted is: mm.

Similarly, the displacement Δx_4 of the hob spindle at the height of H_3 is caused by inclination and bending deformation of the small column (see Fig. 9). So

$$\frac{\Delta S}{2} + \Delta S_2 = \Delta x_4 \tag{47}$$

$$\frac{\Delta x_4}{\Delta x_6} = \frac{H_3}{H_{21}} \Rightarrow \Delta x_4 = \frac{H_3}{H_{21}} \Delta x_6 \tag{48}$$

(a) (b)

Fig. 11. Grating displacement sensor Installation of thermal deformation: (a) Large column bottom; (b) Small column bottom.

(a) (b)

Fig. 12. Grating displacement sensor Installation of thermal deformation: (a) Large column top; (b) Small column top.

where $\Delta S/2$ is the displacement of the hob spindle at the height of H_3 caused by inclination deformation of the small column, ΔS_2 is the displacement of the hob spindle at the height of H_3 caused by bending deformation of the small column, Δx_4 is the displacement of the hob spindle at the height of H_3 caused by inclination and bending deformation of the small column, Δx_6 is the measured value of displacement at the top of the small column. H_{21} is the height of grating displacement sensor to the top surface of the lathe bed(see Fig. 12). Unit adopted is: mm.

From Eqs. (44)-(48) and the analysis above, the displacement of the hob and workpiece spindles at the height of H_3 caused by thermal deformation error Δx of gear hobbing machines is

$$\begin{aligned}\Delta x &= \Delta l + \Delta S + \Delta S_1 + \Delta S_2 \\ &= \Delta x_1 + \Delta x_2 + \Delta x_3 + \Delta x_4\end{aligned}. \tag{49}$$

4.3 Arrangement of experimental apparatus

In the structure of gear hobbing machines, the parts whose temperature is measured need to be covered with heat conductive silicone grease; temperature sensors are placed on top of the silicone grease, and then the temperature sensors are attached by circular magnets. The probes of the grating displacement sensor are upright placed on the end side of parts requiring measurement (in the direction of x-axis of tooth trace deviation). The grating displacement sensor is fixed by the magnetic bracket, which occupies little space. So the effect of the measuring device on the experiment can be omitted. The experimental apparatus is shown in Figs. 10-12.

Table 1. Structural parameter of CNC gear hobbing machines.

Parameter variable	λ /℃	L_1	L_2	L_3	L_4	H_{11}
Numerical value/mm	5.7×10^{-6}	200	565.55	600	50	1073
Parameter variable	L_5	a	b	H	H_3	H_{21}
Numerical value/mm	236.5	700	383	810	524	1322

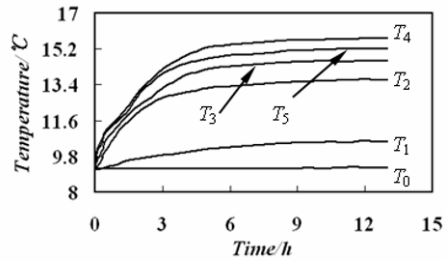

Fig. 13. Testing temperature variety curves of lathe bed.

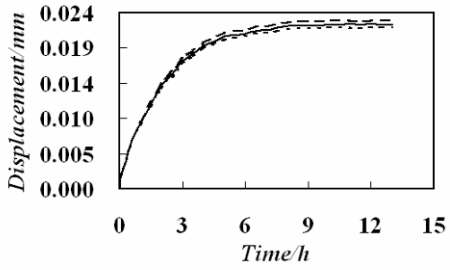

Fig. 14. Thermal deformation displacement variety curves of gear hobbing machine lathe bed: --- $\Delta L/2$ theoretical value, — Δx_1 testing value of displacement at the bottom of inner parts of large columns, － － － Δx_2 testing value of displacement at the bottom of inner parts of small columns.

4.4 The testing data analysis of temperature and displacement

To facilitate comparison between theoretical computation and experimental data, Table 1 shows the parameters of a particular large-scale NC gear hobbing machine of some type. The experimental data of temperature of gear hobbing machine is shown in Figs. 13, 15 and 17. The theoretical value of thermal deformation can be computed through Eq. (42). Both the theoretical value and experimental data are shown in Figs. 14, 16 and 18. The room temperature is 9.12℃, with the precision of 0.01℃, and the test precision of thermal deformation displacement is 0.0001 mm.

The law of thermal deformation of a gear hobbing machine of some type can be obtained from Figs. 13-18. With the same rotation speed, the same set of workpieces is continuously machined in 13 hours. In the previous 4.5 hours, the temperature and the thermal deformation displacement of lathe bed and columns increase rapidly. In the time period between the 4.5 hours and 6 hours, the temperature and displacement of

the lathe bed and column changes slowly, when the gear hobbing machine has almost reached the heat balance. In the sixth hour, the machine is in the state heat balance completely. When in heat balance, the curve of temperature and displacement becomes a horizontal line, that is, the data has little variation.

In Fig. 13, the top surface's temperature is higher than the bottom surface. When in heat balance, the average temperature T_0 of the bottom surface is 9.2℃; the top surface's temperature is 13.96℃. The top surface's temperatures T_4 and T_5 are relatively high, and their average value is 15.76℃ and 15.21℃, respectively. The reasons are that the parts of T_4 and T_5 are not cooled by the cooling liquid, and are heated by the friction heat produced by the drive worktable of worm gear and rails. The deformation data is shown in Fig. 14, in which the experimental data is higher than theoretical values. When the machine tool reaches heat balance, the displacement measured at the bottom end of inner part of large column is 0.009 mm higher than theoretical value, with the relative error of 3.98%. The displacement measured at the bottom end of the inner side of the small column is 0.004 mm higher than theoretical value, with the relative error of 1.84%, which is shown in Table 2. The experimental data is higher than theoretical values; the reason for this result may be the effect of the vibration during cutting and surrounding temperature on the high precision grating displacement sensor.

In Fig. 15, when the machine tool reaches heat balance, the average temperature of the inner side of the large column is 3.64℃ higher than the outer side. The temperatures in the inner side T_7 and T_8 are relatively high, with an average temperature of 14.43℃ and 14.61℃. This is because the place of T_7 and T_8 will be producing the friction heat by cutting workpiece and the Z axis of sliding rails of column and the motor operation and hob spindle of transmission mechanism, making the temperatures of T_7 and T_8 higher than others. The theoretical and experimental data of hob spindle displacement caused by inclination and bending of large column are shown in Fig. 16. When the machine tool reaches the heat balance, the average value of experimental data of hob spindle displacement is 0.0158 mm, the average of theoretical data is 0.0151 mm, so the experimental data is 0.0007 mm higher than theoretical value, with the relative error of 4.43%. The reasons for these are the vibration of machine tool, surrounding temperature, and the warmed cooling liquid passing from the gear cut.

In Fig. 17, when the machine tool reaches heat balance, the average temperature of the inner side of the small column is 3.26℃ higher than outer part. The temperatures in the inner side T_{14} and T_{15} are relatively high, with an average temperature of 14.76℃ and 14.24℃. This is because the place of T_{14} and T_{15} will be producing friction heat by meshing worm gear and worktable rail and the motor operation, making the temperatures of T_{14} and T_{15} higher than others. The theoretical and experimental data of hob spindle displacement caused by inclination and bending of small column are shown in Fig. 18. When the machine tool reaches the heat balance, the average value of experimental data is 0.0215 mm, the average of theoretical data is 0.0207 mm, so the experimental data is 0.0008 mm higher than theoretical value, with a relative error of 3.72%. The reasons for these are the vibration of cutting, surrounding temperature, the warmed cooling liquid and the vibration of rotating worktable.

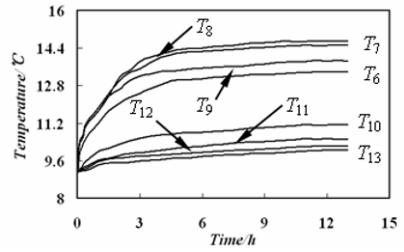

Fig. 15. Experiment temperature variety curves of inner and outer side surface of large column of gear hobbing machine.

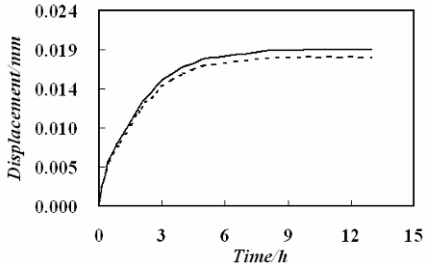

Fig. 16. Thermal deformation displacement of inclination and bending of large column of gear hobbing machine: ----($\Delta S/2+\Delta S_1$) theoretical value, ——— Δx_3 testing value.

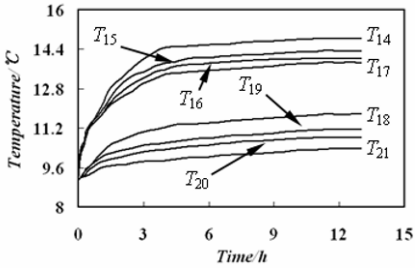

Fig. 17. Experiment temperature variety curves of inner and outer side surface of small column of gear hobbing machine.

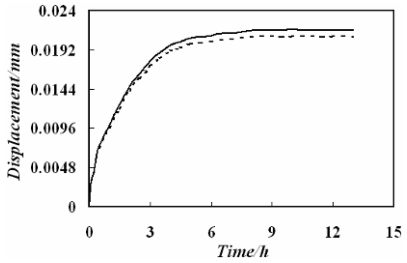

Fig. 18. Thermal deformation displacement of inclination and bend of small column of gear hobbing machine: ----($\Delta S/2+\Delta S_2$) theoretical value, ——— Δx_4 testing value.

Table 2. Compare theory with testing values of heat balance of average thermal deformation displacement of gear hobbing machine.

Average displacement	theoretical value /mm		Testing value /mm		Relative error
Left side of lathe bed	$\triangle L/2$	0.0217	$\triangle x_1$	0.0226	3.98%
Right side of lathe bed	$\triangle L/2$	0.0217	$\triangle x_2$	0.0221	1.81%
Hob spindle	$\triangle S/2+\triangle S_1$	0.0151	$\triangle x_3$	0.0158	4.43%
Workpiece spindle	$\triangle S/2+\triangle S_2$	0.0207	$\triangle x_4$	0.0215	3.72%
Total deviation	$\triangle x$	0.0792	$\triangle x$	0.0821	3.53%

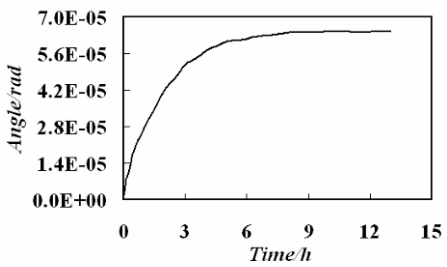

Fig. 19. Deflection angle between hob and workpiece spindles of the centerlines of gear hobbing machine.

From Fig. 19, when the hobbing machine is machining the same batch of workpieces with the same rotating speed, the change law of deflection angle between centerlines of the hob and workpiece spindles is similar with that of thermal displacement. In the 13 hours of cutting, the maximum angle can reach 6.436×10^{-5} rad.

5. The effect of thermal deformation on machining precision

The temperature gradients caused by the uneven temperature distribution make the lathe bed and columns of gear hobbing machines deformed. The displacement caused by thermal deformation increases with the duration of cutting. The position change of cutting point or the distance of centers of the hob and workpiece spindle increases, which produces the tooth trace error and deteriorates the machining precision. From the thermal deformation law, the locus curve of the tooth trace error can be deduced, as is shown in Fig. 21. In the up milling, curve 1 denotes the tooth machining path in ideal conditions. Curve 2 denotes the cutting path before the machine tool reaches the heat balance. This curve shifts to the direction in which the displacement of cutting point increases, which is similar to the change law of the temperature and thermal displacement. The tooth trace error increases with the duration. Curve 3 is the cutting path with the machine tool in heat balance, in which the thermal displacement of the lathe bed and columns vibrates around the average value. The position thermal error reaches the maximum value. The difference

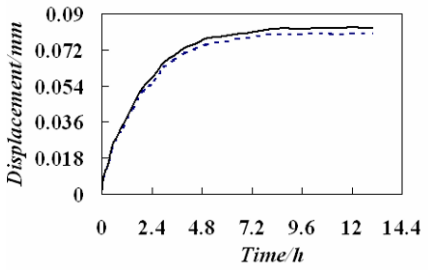

Fig. 20. Total deviation of cutting point position: ---- theoretical value, ——— testing value.

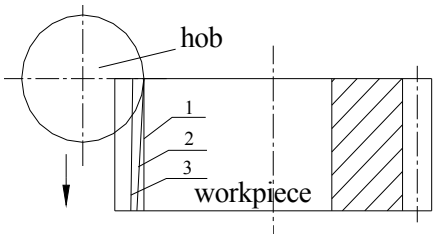

Fig. 21. Tooth traces deviation of cutting gear of gear hobbing machine: 1- ideal machining locus, 2- machining locus before heat balance, 3- machining locus in the heat balance.

between the actual path curve and theoretical curve reaches the maximum value, with the greatest inclination.

From Fig. 20 and Table 2, it is seen that when the machine tool reaches heat balance, the theoretical tooth trace error is 0.0792 mm, the measured one is 0.0821 mm, with the relative error of 3.53%, lower than 5%. So, it is shown that research method applied to this type of gear hobbing machines can have great significance in direction and reference in aspects such as the optimum design of structure, the local temperature control, and prediction and compensation of the tooth trace error.

6. Conclusions

(1) A thermal deformation novel computation model for large scale CNC gear hobbing machines is proposed. Using this model, the deflection angel between centerlines of the hob and workpiece spindle and the total displacement error can be calculated, which reveal the change law of the deformation to cutting time in theory.

(2) The experimental system and platform for thermal deformation study are constructed. The temperature and displacement for some type of gear hobbing machine is tested and analyzed, which reveals the practical law of thermal deformation, and the path curve of tooth trace error and total displacement error are obtained.

(3) By comparison with the theoretically calculated value and experimental data of thermal deformation, the results show the relative error between them is lower than 5%, verifying the novel computation model presented in this paper. Thus, this research holds great significance in direction and reference in aspects such as the optimum design of structure, the

local temperature control, and prediction and compensation of the tooth error.

Acknowledgment

This research was supported by the National Natural Science Funds for Distinguished Young Scholars, China (No. 50925518), the Chongqing Key Scientific Technological Project, China (No. CSTC2011AB3055), the National Key Project for High-end CNC Machine Tools and Basic Manufacturing Equipment, China (No. 2009ZX04001-081), and the National Science and technology of support plan Item, China (No. 2012BAF13B09).

Nomenclature

T	: Temperature or Celsius temperature scale
$\triangle L$	: Deformation of lathe bed
λ	: Coefficient of heat expansion
E	: Elasticity modulus
$\triangle S$	: Deformation of the spindle
H	: Height
B	: Central angle
α	: Rotation angle
ε	: Strain
$\triangle T$	:Temperature difference
k	: Temperature gradient
x	: Distance from any point to center
σ	: Stress
η	: Load ratio
σ_s	: Yielding strength
A	: Area
K	: Stiffness of pull pressure
ξ	: Stiffness ratio
u	: Deformation displacement
$\triangle x$	: Displacement

References

[1] S. R. Park, T. K. Hoang and S. H. Yang, A new optical measurement system for determining the geometrical errors of rotary axis of a 5-axis miniaturized machine tool, *Journal of Mechanical Science and Technology*, 24 (1) (2010) 175-179.

[2] J. Bryan, International status of thermal error research, *Keynote Paper Annals of the CIRP*, 39 (2) (1990) 645-656.

[3] K. Okushima and Y. Kakino, An analysis of methods used in minimizing thermal deformations of machine tools, *Proc. of 16th MTDR Conf* (v16) (1975) 1012-1017.

[4] X. J. Tao and Z. S. Wang, Influence of thermal deformations of the hobbing machine on machining accuracy, *Chinese Journal of Mechanical Transmission*, 29 (3) (2005) 54-57.

[5] Y. Q. Guan, The effect and control of thermal distortions on precision machining, *Chinese Mechanical Research & Application*, 14 (2) (2003) 1-3.

[6] B. F. Ju, J. Z. Fu and Z. C. Chen, Research on the thermal-deformation control by using constant temperature construction of phase change material, *Chinese Journal of Mechanical Engineering*, 36 (6) (2000) 59-63.

[7] Y. T. Fei, *Theory and application of mechanical thermal deformation*, National Defense Industry Press, Beijing, PRC (2009).

[8] Y. Q. Liang, *the basis of the heat transfer and thermal deformation of Machinery Manufacturing*, Machinery Industry Press, Beijing, PRC (1982).

[9] P. J. Ossenbruggen, V. Aggarwal and C. G. Culver, Steel column failure under thermal gradients, *Journal of Structural Division*, ASCE, 99 (ST4) (1973) 727-739.

[10] J. R. Sharples, R. J. Plank and D. A. Nethercot, Load temperature deformation behavior of partially protected steel columns in fires, *Engineering Structures*, 16 (8) (1994) 637-643.

[11] Y. C. Wang, Post-buckling behavior of axially rest rained and axially loaded steel columns under fire conditions, *Journal of Structural Engineering*, ASCE, 130 (3) (2004) 371-380.

[12] G. Q. Li and P. J. Wang, Large deformation analysis of axially re strained beam column under transversely non-uniform temperature distribution in localized fire, *Chinese Quarterly of Mechanics*, 28 (2) (2007) 246-255.

[13] J. P. C. Rodrigues, I. C. Neves and J. C. Valente, Experimental research on the critical temperature of compressed steel element with rest rained thermal elongation, *Fire Safety Journal*, 35 (2) (2000) 77-98.

[14] S. R. Li, C. J. Cheng and Y. H. Zhou, Thermal post-buckling of an elastic beams subjected to a transversely non-uniform temperature rising, *Applied Mathematics and Mechanics*, 24 (5) (2003) 454-460.

[15] D. Mohammada and A. S. Samirb, A new technique for large deflection analysis of non-prismatic cantilever beams, *Mechanics Research Communications*, 32 (6) (2005) 692-703.

Shi-Long Wang received his B.S., M.S. and Ph.D. in Mechanical Engineering from Chongqing University, China, in 1988, 1991 and 1995, respectively. Dr. Wang currently is a Professor at the School of Mechanical Engineering, Chongqing University. He serves as a director of the *Chinese Journal of Mechanical Engineering*. Dr. Wang's research interests include manufacturing automation, CNC machine tool, computer integrated manufacturing and enterprises informatization.

Yong Yang received his M.S. in Vehicle Engineering from Chongqing University, China, in 2007. His Ph.D. degree is in Mechanical Engineering from Chongqing University (2012). Dr. Yang's research interests include CNC machine tool, mechatronics, and manufacturing automation.

Xian-Guang Li received his B.S., M.S. and Ph.D. in Mechanical Engineering from Chongqing University, China, in 1988, 2003 and 2012, respectively. Dr. Li currently is a Professor level senior engineer Chongqing Machine Tool (Group) Co., Ltd., Chongqing, China. Dr. Li's research interests include numerical control technique, CNC machine tool.

Jie Zhou received his B.S. in Mechanical Engineering and his M.S. in Software Engineering from Chongqing University in 1988 and 2007, respectively. Zhou currently is an Associate Professor at the School of Mechanical Engineering, Chongqing University, Chongqing, China. His research interests include manufacturing automation, CNC machine tool and mechatronics.

Ling Kang received her M.S. in Mechanical Engineering from Chingqing University, China, in 2007. She currently is a lecturer at the School of Mechanical Engineering, Chongqing University,. Her research interests include manufacturing automation, CNC machine tool.